Unified Theory of *PT* and *CP* Invariant Topological Metals and Nodal Superconductors

Y. X. Zhao,[1,2,*] Andreas P. Schnyder,[1,†] and Z. D. Wang[2,‡]
[1]*Max-Planck-Institute for Solid State Research, D-70569 Stuttgart, Germany*
[2]*Department of Physics and Center of Theoretical and Computational Physics, The University of Hong Kong, Pokfulam Road, Hong Kong, China*

(Received 29 January 2016; published 14 April 2016)

As *PT* and *CP* symmetries are fundamental in physics, we establish a unified topological theory of *PT* and *CP* invariant metals and nodal superconductors, based on the mathematically rigorous *KO* theory. Representative models are constructed for all nontrivial topological cases in dimensions $d = 1$, 2, and 3, with their exotic physical meanings being elucidated in detail. Intriguingly, it is found that the topological charges of Fermi surfaces in the bulk determine an exotic direction-dependent distribution of topological subgap modes on the boundaries. Furthermore, by constructing an exact bulk-boundary correspondence, we show that the topological Fermi points of the *PT* and *CP* invariant classes can appear as gapless modes on the boundary of topological insulators with a certain type of anisotropic crystalline symmetry.

DOI: 10.1103/PhysRevLett.116.156402

Introduction.—Since the discovery of topological insulators, rapid progress has been made in our understanding of topological band theory [1–3]. Recently, much attention has been paid to topological metals or semimetals, which are characterized by nodal band structures whose stability is guaranteed by certain symmetries and a nontrivial wave function topology [4–7]. The Bloch wave functions of these gapless systems possess a nonzero topological invariant index (e.g., a Chern, winding, or $\mathbb{Z}_2$ number). Thus far, several distinct types of topological semimetals have been explored, including semimetals with Dirac points [8–10], Weyl points [11–13], and Dirac line nodes [14–18]. Experimentally, these topological phases are realized in many different systems. For example, Weyl point nodes have been reported to exist in TaAs [19,20] and NbAs [21], while Dirac line nodes occur in Ca_3P_2 [22], $PbTaSe_2$ [23,24], ZrSiS [25], and carbon allotropes [26,27]. Topological nodal phases have also been created artificially using photonic crystals [28,29] and ultracold atoms in optical lattices [30,31]. Moreover, nodal topological band structures can arise in superconductors with unconventional pairing symmetries [32–34].

In exploring these nodal topological phases, several significant advances have been made recently to classify Fermi surfaces in terms of antiunitary symmetries (e.g., time reversal and particle-hole symmetries) [6,7,35,36], as well as unitary symmetries (e.g., reflection and rotation symmetries) [37–41]. These pieces of work have broadened and deepened our knowledge of symmetry-protected topological materials. However, a unified topological theory of nodal phases that possess the combined symmetry of unitary with antiunitary operations, including a comprehensive classification, is still awaited. In particular, the combined symmetry of time reversal T (or particle-hole C) with inversion P is of fundamental importance. Similar to particle physics, these combined symmetries play fundamental roles in many condensed matter systems, such as centrosymmetric crystal structures, superfluid ^{3}He [4], and possibly some heavy fermion superconductors [42].

In this Letter, we establish a unified theory for the topological properties of *PT* and *CP* symmetry-protected nodal band structures, based on *KO* theory [43–47], i.e., the *K* theory of real vector bundles. Using the homotopy groups of *KO* theory, we topologically classify *PT* and *CP* invariant Fermi surfaces (Table I). Interestingly, in this classification the same *K* groups appear as in the classification of strong topological insulators and superconductors (TIs and TSCs) [47–50], but in a reversed order. We construct concrete models for all topologically nontrivial Fermi surfaces in dimensions $d = 1$, 2, and 3, and elaborate on how the topological charges of the Fermi surfaces in the bulk determine the distribution of topological subgap modes on the boundaries. Furthermore, we show that the *PT* and *CP* invariant topological Fermi points can be reinterpreted as the boundary modes of TIs and TSCs with certain anisotropic crystalline symmetries [specified in Eqs. (16) and (17)], thereby realizing an exact bulk-boundary correspondence.

Topological Fermi surfaces with PT symmetry.—Let us start by considering systems with the combined symmetry

TABLE I. Classification table of *PT* and *CP* invariant Fermi surfaces.

d_c	0	1	2	3	4	5	6	7
$(\hat{P}\hat{T})^2 = +1$	$\mathbb{Z}$	$\mathbb{Z}_2$	$\mathbb{Z}_2$	0	$2\mathbb{Z}$	0	0	0
$(\hat{C}\hat{P})^2 = +1$	$\mathbb{Z}_2$	0	$2\mathbb{Z}$	0	0	0	$\mathbb{Z}$	$\mathbb{Z}_2$
$(\hat{P}\hat{T})^2 = -1$	$2\mathbb{Z}$	0	0	0	$\mathbb{Z}$	$\mathbb{Z}_2$	$\mathbb{Z}_2$	0
$(\hat{C}\hat{P})^2 = -1$	0	0	$\mathbb{Z}$	$\mathbb{Z}_2$	$\mathbb{Z}_2$	0	$2\mathbb{Z}$	0

PT. When a quantum system has both T and P symmetries, the Hamiltonian density $\mathcal{H}(k)$ in momentum space satisfies

$$\hat{T}\mathcal{H}(k)\hat{T}^{-1} = \mathcal{H}(-k) \quad \text{and} \quad \hat{P}\mathcal{H}(k)\hat{P}^{-1} = \mathcal{H}(-k), \quad (1)$$

respectively, where $\hat{T}$ is an antiunitary operator, $\hat{T}i\hat{T}^{-1} = -i$, while $\hat{P}$ is unitary, $\hat{P}i\hat{P}^{-1} = i$. In this work we only require the combined symmetry $A = PT$ for the topological stability, while perturbations breaking both T and P but preserving PT are allowed. $A = PT$ is antiunitary, $\hat{A}i\hat{A}^{-1} = -i$, acting on $\mathcal{H}(k)$ as

$$\hat{A}\mathcal{H}(k)\hat{A}^{-1} = \mathcal{H}(k). \quad (2)$$

It is important to observe that the symmetry PT operates trivially in momentum space, which motivates our classification strategy, namely, (i) to determine the topological space of the Hamiltonians pointwisely in k space and (ii) to classify the topological configurations of $\mathcal{H}(k)$ on the d_c-dimensional sphere S^{d_c} enclosing the gapless region. Here, $d_c = d - d_{\mathrm{FS}} - 1$ for a d_{FS}-dimensional Fermi surface in d-dimensional k space. These two steps can be performed by use of the theory of *real* Clifford algebras and KO theory, respectively. The details of these mathematical derivations are given in the Supplemental Material (SM) [51]. Because of the antiunitarity of $\hat{A}$, we treat the imaginary unit i as an operator [51,52], which allows us to construct a Clifford algebra with the three generators, $\hat{A}$, $i\hat{A}$, and $i\mathcal{H}$, and the anticommutators,

$$\{\hat{A}, i\hat{A}\} = 0, \qquad \{\hat{A}, i\mathcal{H}\} = 0, \qquad \{i\mathcal{H}, i\hat{A}\} = 0. \quad (3)$$

Assuming that the chemical potential $\mu = 0$, it is sufficient for our topological purpose to study flattened Hamiltonians $\tilde{\mathcal{H}}(k)$, whose band spectra are normalized such that $\tilde{\mathcal{H}}^2(k) = 1$ for every point k where the spectrum is gapped. With this normalization, the squares of the above generators are given by

$$(i\mathcal{H})^2 = -1, \qquad \hat{A}^2 = (i\hat{A})^2 = \pm 1, \quad (4)$$

where $\hat{A}^2 = (i\hat{A})^2$ due to the antiunitarity of $\hat{A}$.

We first consider $\hat{A}^2 = +1$, in which case both $\hat{A}$ and $i\hat{A}$ are positive, generating the Clifford algebra $C^{0,2}$, which is further extended to $C^{1,2}$ by the negative generator $i\mathcal{H}$. In other words, the topological space of all PT invariant $\mathcal{H}$ is determined by all possible Clifford algebra extensions from $C^{0,2}$ to $C^{1,2}$. Since the extension $C^{0,2} \subset C^{1,2}$ is equivalent to $C^{0,0} \subset C^{0,1}$, the topological space is equivalent to R_0, the zeroth classifying space of KO theory [43–45]. According to our classification strategy, we next need to classify the topological configurations of R_0 on the sphere S^{d_c}. To do so, we note that since the trivial action of PT in k space corresponds to the trivial involution of KR theory, the classification is given by KO theory, the simplest instance of KR theory. Hence, the classification of PT invariant Fermi surfaces with $\hat{A}^2 = +1$ follows from the KO groups

$$\tilde{KO}(S^{d_c}) \cong \mathbb{Z}, \mathbb{Z}_2, \mathbb{Z}_2, 0, 2\mathbb{Z}, 0, 0, 0, \quad (5)$$

with $d_c \equiv 0, 1, \ldots, 7 \bmod 8$, and $\tilde{KO} = \tilde{KO}^{-0}$, where "0" is determined by the classifying space R_0.

Second, we consider $\hat{A}^2 = -1$, in which case $\hat{A}$ and $i\hat{A}$ generate the Clifford algebra $C^{2,0}$, which is extended by $i\mathcal{H}$ to $C^{3,0}$. From $C^{2,0} \subset C^{3,0} \approx C^{0,4} \subset C^{0,5}$, it follows that the topological space of Hamiltonians is given by R_4. Thus, the classification of Fermi surfaces with codimension $(d_c + 1)$ and $\hat{A}^2 = -1$ is

$$\tilde{KO}^{-4}(S^{d_c}) \cong 2\mathbb{Z}, 0, 0, 0, \mathbb{Z}, \mathbb{Z}_2, \mathbb{Z}_2, 0, \quad (6)$$

with $d_c \equiv 0, 1, \ldots, 7 \bmod 8$.

Topological Fermi surfaces with CP symmetry.—Next, we look into CP symmetric Fermi surfaces (or superconducting nodes). C is implemented by an antiunitary operator $\hat{C}$, which acts on the Hamiltonian as

$$\hat{C}\mathcal{H}(k)\hat{C}^{-1} = -\mathcal{H}(-k). \quad (7)$$

Accordingly, we need to consider the Clifford algebra generated by $\hat{B} = \hat{C}\hat{P}$, $\mathcal{H}$, and $i\hat{B}$ with the anticommutators

$$\{\hat{B}, \mathcal{H}\} = 0, \qquad \{\hat{B}, i\hat{B}\} = 0, \qquad \{\mathcal{H}, i\hat{B}\} = 0. \quad (8)$$

As before, we normalize the band spectrum such that

$$\mathcal{H}^2 = 1, \qquad \hat{B}^2 = (i\hat{B})^2 = \pm 1. \quad (9)$$

For $\hat{B}^2 = +1$, one can find that the Hamiltonian space is equivalent to R_2 [51], corresponding to the Clifford algebra extension $C^{0,2} \subset C^{0,3}$. From this it follows that the classification is given by

$$\tilde{KO}^{-2}(S^{d_c}) \cong \mathbb{Z}_2, 0, 2\mathbb{Z}, 0, 0, 0, \mathbb{Z}_2, \mathbb{Z}, \quad (10)$$

with $d_c \equiv 0, 1, \ldots, 7 \bmod 8$. For $\hat{B}^2 = -1$, on the other hand, the Hamiltonian space is R_6, corresponding to $C^{2,0} \subset C^{2,1} \approx C^{0,6} \subset C^{0,7}$. This leads to the classification

$$\tilde{KO}^{-6}(S^{d_c}) \cong 0, 0, \mathbb{Z}, \mathbb{Z}_2, \mathbb{Z}_2, 0, 2\mathbb{Z}, 0, \quad (11)$$

with $d_c \equiv 0, 1, \ldots, 7 \bmod 8$. This concludes the derivation of the classification, as summarized in Table I.

Several comments are in order. First, note that all classifications are given by $\tilde{KO}^{-q}(S^{d_c})$, where q is even and denotes the index of the classifying space R_q [53]. Second, in the present classification, the K groups as a function of d_c appear in reverse order compared to the tenfold classification of Fermi surfaces and strong TIs and TSCs [47]. Third, if we replace d_c by the spatial dimension d, KO theory yields the classification of PT and CP

invariant TIs and TSCs, since PT and CP act trivially in momentum space [50]. Note, however, that these TIs and TSCs do not exhibit any symmetry-protected surface states, since the boundary breaks $PT(CP)$. Finally, we emphasize that the classification relies only on the combined symmetry $PT(CP)$. Both P and $T(C)$ may be broken individually, but the combination must be preserved, which is in contrast to previous studies of P-symmetric systems [38].

Representative models.—We now construct representative models for all nontrivial cases of the classification in the physical dimensions $d = 1$, 2, and 3. (The computation of the corresponding topological charges is presented in the SM [51]). Discussing the symmetry classes in the same sequence as before, we start with the symmetry class $\hat{A}^2 = (PT)^2 = +1$, for which there exist topologically nontrivial Fermi surfaces in all physical dimensions, since for $d_c = 0$, 1, and 2 the classification is given by $\mathbb{Z}$, $\mathbb{Z}_2$, and $\mathbb{Z}_2$, respectively. The case $d_c = 0$ simply corresponds to Fermi surfaces of spinless free fermions in any dimension d; see Refs. [51,54]. The case $d_c = 1$ corresponds to topological Fermi points (lines) in 2D (3D) with $\mathbb{Z}_2$ topological charge. For 2D, a simple model can be constructed with rank-2 matrices. We choose $\hat{T} = \hat{\mathcal{K}}$ and $\hat{P} = \sigma_3$, which yields $\hat{A} = \sigma_3\hat{\mathcal{K}}$ and $[\hat{T}, \hat{P}] = 0$, where $\hat{\mathcal{K}}$ denotes the complex conjugate operator and σ_j's are Pauli matrices. (Alternatively, one can consider $\hat{T} = -i\sigma_2\hat{\mathcal{K}}$ and $\hat{P} = \sigma_1$ with the anticommutation relation $\{\hat{T}, \hat{P}\} = 0$). Thus, the general form of the Hamiltonian is $\mathcal{H}_0 = f_1(k)\sigma_2 + f_2(k)\sigma_3$, with f_i arbitrary functions of k, since PT merely forbids the σ_1 term. For concreteness, let us choose

$$\mathcal{H}_0 = k_x\sigma_2 + (k_y^2 - R^2)\sigma_3, \tag{12}$$

with the constant $R \sim 1$. $\mathcal{H}_0$ exhibits two Dirac points at $k = (0, \pm R)$ with topological charges $\nu = \pm 1$. The low-energy physics in the vicinity of these two gapless points is described by the Dirac-type Hamiltonian $\mathcal{H}_\pm = k_x\sigma_2 \pm k_y\sigma_3$, whose stability is guaranteed by a quantized Berry phase [51,55]. Note that $\mathcal{H}_0$ has both T and P symmetries. However, the Dirac points cannot be gapped out by P and T breaking perturbations that satisfy PT, such as $\mathcal{H}' = \mu\sigma_0 + (\eta + \epsilon_1 k_x^2)\sigma_2 + \epsilon_2 k_y\sigma_3$. These perturbations only change the local properties of the Dirac points, e.g., position and dispersion, but do not open a full gap. We emphasize that the $\mathbb{Z}_2$ Fermi points of $\mathcal{H}_0$ are fundamentally different from those with $\mathbb{Z}$ classification in symmetry class AIII, although in both cases σ_1 terms are symmetry forbidden. To illustrate the $\mathbb{Z}_2$ nature of the Fermi points, we consider a doubled version of $\mathcal{H}_0$, namely, $\mathcal{H}_0 \otimes \tau_0$. It is found that there are PT-preserving perturbations, for instance, $m\sigma_1 \otimes \tau_2$, that open up a full gap. However, all of these gap opening perturbations are forbidden by chiral symmetry. Hence, the discussed $\mathbb{Z}_2$ Fermi points are clearly distinct from the $\mathbb{Z}$ Fermi points of class AIII [6,7,35]. A lattice version of Eq. (12), $\mathcal{H}(k) = \sin k_x\sigma_2 + (\lambda - \cos k_y)$ $(|\lambda| < 1)$, will be discussed in detail later. It is also noted that $\mathcal{H}_0$ can straightforwardly be extended to a 3D case with a nontrivial nodal loop [51].

Next, we consider the case $\hat{A}^2 = +1$ with $d_c = 2$. According to Table I, there exist in this symmetry class PT-preserving Fermi points in $d = 3$ with a $\mathbb{Z}_2$ charge. A minimal model for these $\mathbb{Z}_2$ Dirac points can be constructed by rank-4 matrices. Choosing $\hat{A} = \sigma_3 \otimes \tau_0\hat{\mathcal{K}}$, we find that the following continuum model exhibits such a Dirac point:

$$\mathcal{H}_D(k) = k_x\sigma_1 \otimes \tau_2 + k_y\sigma_2 \otimes \tau_0 + k_z\sigma_3 \otimes \tau_0, \tag{13}$$

where τ_j's are a second set of Pauli matrices. Observe that the two independent mass matrices $\sigma_1 \otimes \tau_3$ and $\sigma_1 \otimes \tau_1$ are forbidden by PT symmetry. However, the Fermi point of the doubled Hamiltonian $\mathcal{H}_D \otimes \kappa_0$ can be gapped out by the mass terms $m\sigma_1 \otimes \tau_1 \otimes \kappa_2$ and $m\sigma_1 \otimes \tau_3 \otimes \kappa_2$, with κ_j's being Pauli matrices, which illustrates the $\mathbb{Z}_2$ nature of the Dirac point of $\mathcal{H}_D$.

For symmetry class $\hat{A}^2 = -1$, the only nontrivial case in $d = 1$, 2, or 3 is $d_c = 0$, which has a $2\mathbb{Z}$ classification (Table I). This simply corresponds to spinful free fermions. Choosing $\hat{T} = i\sigma_2\hat{\mathcal{K}}$ and $\hat{P} = \sigma_0$, which yields $\hat{A} = i\sigma_2\hat{\mathcal{K}}$ and $[\hat{T}, \hat{P}] = 0$, the spinful free-fermion Hamiltonian is given by $\mathcal{H}^s_{\text{free}} = k^2/2m\sigma_0 - \mu\sigma_0$. Note that all spin-orbit coupling terms involving σ_j $(j = 1, 2, 3)$ are excluded by PT symmetry.

Let us now turn to nodal band structures with CP symmetry. For symmetry class $\hat{B}^2 = (CP)^2 = +1$ with $d_c = 0$, there exist nodes with a $\mathbb{Z}_2$ classification. To construct a representative model, we choose $\hat{C} = \tau_1\hat{\mathcal{K}}$ and $\hat{P} = i\tau_2$, so that $\hat{B} = \tau_3\hat{\mathcal{K}}$. Since the only Pauli matrix that anticommutes with $\hat{B}$ is τ_1, we find that the continuum model is $\mathcal{H}(k) = k\tau_1$ in 1D. It is obvious that the mass terms $m\tau_2$ and $m\tau_3$ are forbidden by CP symmetry. To see the $\mathbb{Z}_2$ nature of the Fermi point, we observe that the doubled Hamiltonian $\tilde{\mathcal{H}}(k) = k\tau_1 \otimes \sigma_0$ with the trivial $\mathbb{Z}_2$ charge can be gapped by the CP invariant terms $m\tau_3 \otimes \sigma_2$ and $m\tau_2 \otimes \sigma_2$. Models of these CP invariant nodes in 2D and 3D can be constructed in an analogous manner.

For $\hat{B}^2 = +1$ and $d_c = 2$, there is a $2\mathbb{Z}$ classification. A representative model can be constructed by 4×4 matrices. Choosing $\hat{B} = \tau_3 \otimes \sigma_0\hat{\mathcal{K}}$, the continuum Hamiltonian is given by

$$\mathcal{H}_W^{\text{double}} = k_x\tau_1 \otimes \sigma_1 + k_y\tau_0 \otimes \sigma_2 + k_z\tau_1 \otimes \sigma_3, \tag{14}$$

since there are only three mutually anticommuting 4×4 matrices that also anticommute with $\hat{B}$. $\mathcal{H}_W^{\text{double}}$ exhibits a double Weyl point at $k = 0$ with topological charge $\nu = 2$, which is defined in terms of a Chern number on a sphere enclosing the Weyl point [51,56]. Despite its similar appearance, this model should be distinguished from the

Dirac Hamiltonian Eq. (13) that has a vanishing Chern number. The remaining nontrivial case in physical dimensions is $d_c = 2$ for $\hat{B}^2 = -1$, which may be exemplified by a Weyl point [51].

In passing, we note that the A phase of ^{3}He can be viewed as an example of CP symmetry-protected nodal points. ^{3}He-A has both C and P symmetry with $\hat{C} = i\sigma_2 \otimes i\tau_2\hat{\mathcal{K}}$ and $\hat{P} = \tau_3$, respectively, which yields $(\hat{C}\hat{P})^2 = -1$ [4]. Thus, according to Table I the classification of the ^{3}He $-$ A point nodes is of $\mathbb{Z}$ type with a topological charge of ± 2, due to spin degeneracy. CP invariant perturbations, such as spin-orbit coupling, may split the spin degeneracy, which divides the doubly charged Weyl points into Weyl points with charge one. This is in contrast to the elementary Fermi point of Eq. (14), which has a $2\mathbb{Z}$ classification.

Bulk-boundary correspondences.—The distribution of subgap states at the boundary of topological metals or semimetals is determined by the topological charges of the Fermi surfaces in the bulk. This is illustrated in Fig. 1(a), which shows how a small sphere S^2 (or circle S^1) enclosing the bulk gapless region may be deformed continuously into two large S^2's (S^1's) in the Brillouin zone (BZ) due to the periodicity in k. By regarding these large S^2's (S^1's) as subsystems of the whole system, we obtain the following relation:

$$\nu = N_R - N_L, \tag{15}$$

where ν is the topological charge of the Fermi surface and $N_{R/L}$ are the topological numbers on the right or left S^2 (S^1). Since PT (CP) acts trivially in k, all three topological indexes N_R, N_L, and ν belong to the same symmetry class of Table I. Therefore, Eq. (15) determines the number of subgap modes on the boundaries that are perpendicular to the subsystems $S^2_{R/L}$ ($S^1_{R/L}$). In general, there may exist several topologically charged gapless regions in the BZ, which leads to a set of equations of the form Eq. (15) that determines the distribution of the boundary modes [57].

To illustrate the above bulk-boundary correspondence, we discuss the gapless modes on the (11) and (01) edges of

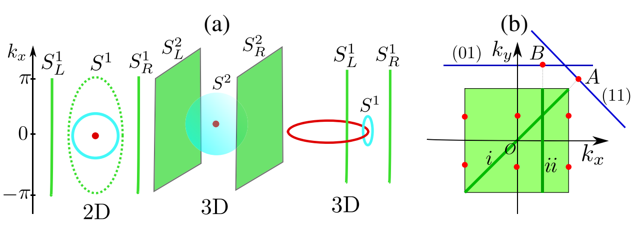

FIG. 1. (a) A small sphere (circle) (cyan) enclosing the gapless point (ring) (red) can be deformed into two large spheres (circles) (green) in the BZ. Note that the BZ is periodic in k. (b) Lattice model with topological Fermi points (red) in its bulk BZ (light green). The boundary BZs for the (11) and (01) edges are indicated by blue lines.

the lattice model of Eq. (12) [see Fig. 1(b)]. Consider point A on the (11) edge BZ, which can be viewed as an end point of the 1D subsystem i. Since i encloses an odd number of nontrivial $\mathbb{Z}_2$ Fermi points, it has a nontrivial topological index given by the geometric phase of the Berry connection. Hence, a subgap state appears at the end point A. In contrast, no edge state appears at point B of the (01) edge BZ, since B is the end point of the subsystem ii, which encloses an even number of nontrivial $\mathbb{Z}_2$ Fermi points leading to a trivial topological index. This bulk-boundary correspondence can be utilized in experiments to identify PT (CP) invariant materials. In the SM [51] we present an explicit calculation of these topological indices, confirming the above analyses [58].

In closing, we note that by use of a bulk-boundary correspondence analysis, the topological Fermi surfaces of Table I can be interpreted as gapless boundary modes of fully gapped TIs and TSCs with certain crystalline symmetries. To demonstrate this, let us consider a gapless dD boundary of a $(d+1)$D fully gapped TI and TSC. Since the gapped bulk of the TIs and TSCs provides a physical ultraviolet cutoff for the gapless boundary modes, the nontrivial topological configuration of the TIs and TSCs imprints itself on the ultraviolet behavior of the boundary modes. To make this more explicit, let us assume that the gapless boundary modes are Fermi points with codimension $d_c = d - 1$. The topological charge of these Fermi points is determined by invariants that are defined on $(d-1)$D spheres S^{d-1} enclosing the Fermi points. In order to establish a correspondence between the topological charge of the boundary modes and the bulk topology of the $(d+1)$D TIs and TSCs, one must show that the two have the same classifications, i.e., that the two classifications are mapped onto each other by a two-dimension shift. For the strong TIs and TSCs of the tenfold way, such a two-dimension shift arises since the involution due to T or C is different for the S^{d_c} spheres enclosing the boundary modes and the bulk k space of the TIs and TSCs [35,51,59]. For PT and CP symmetries, however, there is no such involution difference between S^{d_c} and the bulk k space of the TIs and TSCs. Hence, the PT (CP) invariant Fermi surfaces of Table I must be related to TIs and TSCs with a symmetry different from PT (CP). Indeed, we find that the classification of Table I is related to the classification of $(d+1)$D gapped band structures with the antiunitary symmetries $D = TR$ and $E = CR$, where R acts on the TIs or TSCs as

$$\hat{R}\mathcal{H}_{TI}(k, k_{d+1})\hat{R}^{-1} = \mathcal{H}_{TI}(-k, k_{d+1}), \tag{16}$$

and D and E restrict $\mathcal{H}_{TI}(k, k_{d+1})$ as

$$\begin{aligned}\hat{D}\mathcal{H}_{TI}(k, k_{d+1})\hat{D}^{-1} &= \mathcal{H}_{TI}(k, -k_{d+1}),\\ \hat{E}\mathcal{H}_{TI}(k, k_{d+1})\hat{E}^{-1} &= -\mathcal{H}_{TI}(k, -k_{d+1}).\end{aligned} \tag{17}$$

Note that R projected onto the boundary acts like an inversion symmetry in the boundary BZ. The classification of TIs and TSCs with symmetry Eq. (17) is given by KR theory as $KR^{-q}(B^{1,d}, S^{1,d})$. It follows from the relation [43,46]

$$KR^{-q}(B^{1,d}, S^{1,d}) \cong \tilde{KO}^{-q}(S^{d-1}) \tag{18}$$

that PT (CP) symmetric Fermi surfaces with codimension $d_c = d - 1$ have the same classification as $(d+1)$D TIs and TSCs with symmetry Eq. (17), which establishes the promised exact bulk-boundary correspondence.

We thank A. J. Leggett for helpful discussions. This work was partially supported by the GRF of Hong Kong (Grants No. HKU173051/14P and No. HKU173055/15P).

*y.zhao@fkf.mpg.de
†a.schnyder@fkf.mpg.de
‡zwang@hku.hk

[1] M. Z. Hasan and C. L. Kane, Rev. Mod. Phys. **82**, 3045 (2010).
[2] X.-L. Qi and S.-C. Zhang, Rev. Mod. Phys. **83**, 1057 (2011).
[3] C.-K. Chiu, J. C. Y. Teo, A. P. Schnyder, and S. Ryu, arXiv:1505.03535.
[4] G. E. Volovik, *Universe in a Helium Droplet* (Oxford University Press, Oxford, 2003), ISBN:.
[5] P. Hořava, Phys. Rev. Lett. **95**, 016405 (2005).
[6] Y. X. Zhao and Z. D. Wang, Phys. Rev. Lett. **110**, 240404 (2013); **114**, 206602 (2015).
[7] S. Matsuura, P.-Y. Chang, A. P. Schnyder, and S. Ryu, New J. Phys. **15**, 065001 (2013).
[8] Z. K. Liu *et al.*, Nat. Mater. **13**, 677 (2014).
[9] M. Neupane *et al.*, Nat. Commun. **5**, 4786 (2014).
[10] S.-Y. Xu *et al.*, Science **347**, 294 (2015).
[11] X. Wan, A. M. Turner, A. Vishwanath, and S. Y. Savrasov, Phys. Rev. B **83**, 205101 (2011).
[12] P. Hosur and X. Qi, C.R. Phys. **14**, 857 (2013).
[13] O. Vafek and A. Vishwanath, Annu. Rev. Condens. Matter Phys. **5**, 83 (2014).
[14] C. Fang, Y. Chen, H.-Y. Kee, and L. Fu, Phys. Rev. B **92**, 081201 (2015).
[15] C.-K. Chiu and A. P. Schnyder, J. Phys. Conf. Ser. **603**, 012002 (2015).
[16] Y.-H. Chan, C.-K. Chiu, M. Y. Chou, and A. P. Schnyder, arXiv:1510.02759.
[17] Y. Kim, B. J. Wieder, C. L. Kane, and A. M. Rappe, Phys. Rev. Lett. **115**, 036806 (2015).
[18] R. Yu, H. Weng, Z. Fang, X. Dai, and X. Hu, Phys. Rev. Lett. **115**, 036807 (2015).
[19] S.-Y. Xu *et al.*, Science **349**, 613 (2015).
[20] B. Q. Lv *et al.*, Phys. Rev. X **5**, 031013 (2015).
[21] S.-Y. Xu *et al.*, Nat. Phys. **11**, 748 (2015).
[22] L. S. Xie, L. M. Schoop, E. M. Seibel, Q. D. Gibson, W. Xie, and R. J. Cava, APL Mater. **3**, 083602 (2015).
[23] M. N. Ali, Q. D. Gibson, T. Klimczuk, and R. J. Cava, Phys. Rev. B **89**, 020505 (2014).
[24] G. Bian *et al.*, arXiv:1505.03069.
[25] L. M. Schoop, M. N. Ali, C. Straßer, V. Duppel, S. S. P. Parkin, B. V. Lotsch, and C. R. Ast, arXiv:1509.00861.
[26] K. Mullen, B. Uchoa, and D. T. Glatzhofer, Phys. Rev. Lett. **115**, 026403 (2015).
[27] Y. Chen, Y. Xie, S. A. Yang, H. Pan, F. Zhang, M. L. Cohen, and S. Zhang, Nano Lett. **15**, 6974 (2015).
[28] L. Lu, L. Fu, J. D. Joannopoulos, and M. Soljacic, Nat. Photonics **7**, 294 (2013).
[29] L. Lu, Z. Wang, D. Ye, L. Ran, L. Fu, J. D. Joannopoulos, and M. Soljačić, Science **349**, 622 (2015).
[30] D.-W. Zhang, Y. X. Zhao, R.-B. Liu, Z.-Y. Xue, S.-L. Zhu, and Z. D. Wang, arXiv:1601.00371; Phys. Rev. A (to be published).
[31] K. Sun, W. V. Liu, A. Hemmerich, and S. Das Sarma, Nat. Phys. **8**, 67 (2012).
[32] S. A. Yang, H. Pan, and F. Zhang, Phys. Rev. Lett. **113**, 046401 (2014).
[33] A. P. Schnyder and P. M. R. Brydon, J. Phys. Condens. Matter **27**, 243201 (2015).
[34] S. Kobayashi, K. Shiozaki, Y. Tanaka, and M. Sato, Phys. Rev. B **90**, 024516 (2014).
[35] Y. X. Zhao and Z. D. Wang, Phys. Rev. B **89**, 075111 (2014).
[36] Y. X. Zhao and Z. D. Wang, Phys. Rev. Lett. **116**, 016401 (2016).
[37] C.-K. Chiu and A. P. Schnyder, Phys. Rev. B **90**, 205136 (2014).
[38] K. Shiozaki and M. Sato, Phys. Rev. B **90**, 165114 (2014).
[39] M. Koshino, T. Morimoto, and M. Sato, Phys. Rev. B **90**, 115207 (2014).
[40] B.-J. Yang and N. Nagaosa, Nat. Commun. **5**, 5898 (2014).
[41] Z. Gao, M. Hua, H. Zhang, and X. Zhang, arXiv:1507.07504 [Phys. Rev. B (to be published)].
[42] C. Pfleiderer, Rev. Mod. Phys. **81**, 1551 (2009).
[43] M. F. Atiyah, Q. J. Math. **17**, 367 (1966).
[44] M. Karoubi, *K-Theory. An Introduction* (Springer, New York, 1978).
[45] M. F. Atiyah, R. Bott, and A. Shapiro, Topology **3**, 38 (1964).
[46] M. Atiyah, *K-Theory* (Westview Press, Boulder, 1994).
[47] This is due to the involution difference of the symmetry operations in momentum space:PT and PC symmetries leave k fixed, whereas T and C map k to $-k$. The classifications in the real Altland-Zirnbauer classes are given by the KR theory with the involution of k to $-k$, while the KO theory is just the simplest case of the KR theory with trivial involution.
[48] A. Kitaev, AIP Conf. Proc. **1134**, 22 (2009).
[49] A. P. Schnyder, S. Ryu, A. Furusaki, and A. W. W. Ludwig, Phys. Rev. B **78**, 195125 (2008).
[50] S. Ryu, A. P. Schnyder, A. Furusaki, and A. W. W. Ludwig, New J. Phys. **12**, 065010 (2010).
[51] See Supplemental Material at http://link.aps.org/supplemental/10.1103/PhysRevLett.116.156402 for the mathematical basics of real Clifford algebras and of the KO theory, for details of the considered models, for the computation of topological charges, and for the details of the lattice model of Eq. (12).
[52] T. Morimoto and A. Furusaki, Phys. Rev. B **88**, 125129 (2013).

[53] In principle, symmetry classes with odd q may also be defined, which would lead to an eightfold periodicity of the classification with respect to both q and d_c.

[54] For the classification $\mathbb{Z}$, the topological charge is just given by the Chern number, which actually requires no symmetry.

[55] Nodal points protected by PT symmetry are also realized in two-band Hamiltonians with the symmetry operators $\hat{A} = \sigma_{1,0}\hat{\mathcal{K}}$, whose low-energy continuum description reads $H_{2,3} = (k_x - K_x)\sigma_1 + (k_y - K_y)\sigma_{2,3}$, where $\mathbf{K} = (K_1, K_2)$ denotes the position of the nodal point. The Hamiltonian H_2 describes the two Dirac points in graphene ($\hat{P} = \sigma_1$, $\hat{T} = \hat{\mathcal{K}}$), while H_3 has recently been realized in the cold atom experiment of Ref. [60], although in that work the exotic PT-invariant $\mathbb{Z}_2$ topology was not recognized.

[56] Note that spin-degenerate Weyl points described by $\mathcal{H}_W = \sigma_0 \otimes \tau \cdot \mathbf{k}$, with the CP symmetry given by $\hat{C}\hat{P} = \sigma_2 \otimes \tau_2\hat{\mathcal{K}}$, belong to the same symmetry class as that of Eq. (14). These spin-degenerate Weyl points may be realized in carbon allotropes [27].

[57] Note that the bulk classification of Table I, for which we have assumed that any boundary is at the asymptotic infinity (cf. Ref. [4]), is not spoiled by the P symmetry breaking at the boundary.

[58] S. Q. Shen, *Topological Insulators: Dirac Equation in Condensed Matters* (Springer, New York, 2013).

[59] Y. X. Zhao and Z. D. Wang, Phys. Rev. B **90**, 115158 (2014).

[60] L. Huang *et al.*, Nat. Phys., DOI: 10.1038/nphys3672 (2016).